SID

SOCIETY FOR INFORMATION DISPLAY

CONFERENCE RECORD OF THE

1997

INTERNATIONAL DISPLAY RESEARCH CONFERENCE

SEPTEMBER 15–19, 1997
TORONTO, CANADA

Featuring
International Workshops
on
LCD Technology
and
Emissive Technology

Sponsored by
The Society for Information Display

In cooperation with
The IEEE Electron Devices Society

INTEGRATED ORGANIC LIGHT EMITTING DIODE STRUCTURES USING DOPED POLYMERS

J.C. Sturm and C.C. Wu

Center for Photonic and Optoelectronic Materials, Department of Electrical Engineering, Princeton University, Princeton, NJ 08544 USA sturm@ee.princeton.edu

Abstract

In this work we describe the development of single-organic-layer LED's based on doped-polymers which have high efficiency (> 1% quantum efficiency measured out the back of the glass) and low drive voltage (< 10 V at 100 cd/m^2). The LED's are based on poly (N-vinylcarbazole) (PVK), into which various electron transport agents and emitting centers have been doped for red, green and blue emission. Proper ITO surface preparation is crucial for achieving low turn-on voltages. We will then use these LED's as model systems for the integration of multiple spin-coated organic layers onto a single substrate (for integrated red, green, and blue emitters) and for the integration of OLED's and amorphous silicon TFT's on novel substrates.

Introduction

For an organic light emitting diode display products, it is necessary not only to have an OLED with good performance, but integration issues must also be considered. In this paper we describe first how doped blends of PVK can be used to fabricate OLED's with good performance with only a single organic layer. To achieve good device performance both optimization of the organic materials and the interfaces is required. By using dry-etching to pattern the organic layers, three different spin-coated organics can be integrated onto a single substrate for full color demonstration. Finally, thin stainless steel foils are used as substrates not only to demonstrate the integration of OLED's with amorphous silicon TFT's, but also to demonstrate a new class of rugged lightweight substrates.

Doped Polymers

It is difficult to find an organic material with optimum hole transport, electron transport, and light emission properties. In OLED's based on small molecules, which are typically deposited by evaporation, these different functions are usually separated into different layers. Polymer are usually deposited by wet-coating techniques, such as the spin-coating used in this work. Because the carrier solvent of a second layer usually will dissolve any previously deposited layers, making such layered structures with polymers is difficult. An alternative approach is to combine the various hole transport, electron transport, and emissive materials in solution, and deposit all materials in a single layer in a blend (assuming no phase segregation occurs).

While this approach to OLED's is well known [1-6], previous approaches have generally been limited by high drive voltages (> 30 V) and/or low quantum efficiencies (<0.1%). Our work is based on PVK, which is a relatively good hole transport

ISSN1083-1312/97/1701-F011-$1.00 + .00 © 1997 SID

polymer, but is only a weak emitter of light in the deep blue (pure PVK OLED's in our lab emit at 430 nm with an efficiency < 0.1%.) Adding dyes to the PVK increases both photoluminescence (PL) and electroluminescence (EL) efficiencies because of the high radiative probabilities of the dyes and because excitons become localized on the dyes and cannot migrate to non-radiative centers. Fig. 1 shows the spectra and Fig. 2 the integrated PL intensity for 340 nm excitation as a function of the content of Bu-PPyV in PVK. Bu-PPyV is a fluorescent polymer which emits in the green in low concentrations and in the red at high concentrations (due to excimers) [7] .

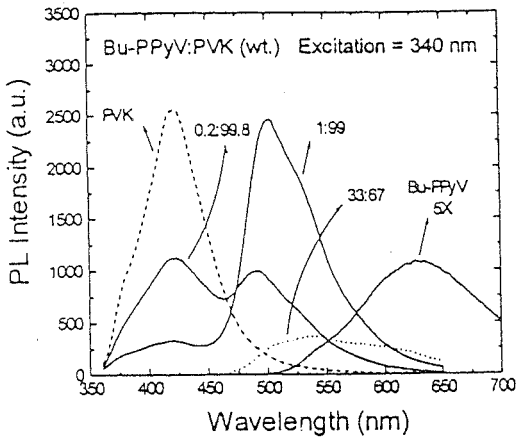

Fig. 1. PL spectra of Bu-PPyV:PVK blend thin films with 340 nm excitation showing PPyV monomer emission at low concentrations and excimer emission at high concentrations. Concentration fractions are calculated by weight. [9]

These films, and all others in this paper, were deposited by spin coating using chloroform. Qualitatively similar PL results are obtained for either two-component (PVK/Bu-PPyV) or three component (PVK/PBD/Bu-PPyV) blends. (PBD is a well known small molecule electron transport agent which was added to the blends in solution before spin-coating [8]. Note efficient energy transfer is achieved between the PVK, where most absorption occurs, and the dye, so that at 1% (weight) dye concentration almost no emission from the PVK can be seen.

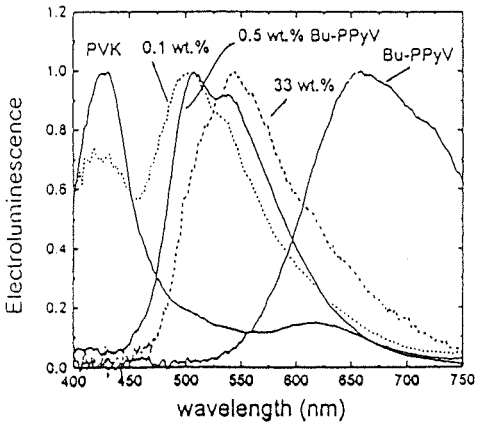

Fig. 2. Normalized EL spectra of ITO:PVK:Bu-PPyV/Mg:Ag/Ag devices for various Bu-PPyV contents [9].

Devices were fabricated from these blends by depositing the films by spin-coating on ITO-coated glass, followed by Mg:Ag/Ag evaporated contacts. External EL efficiencies were determined by measuring only the light emitted out the back of the glass. Fig. 2 shows PL spectra for different dye content, showing the same gradual trend of the PL of going from a weak PVK emission to a stronger Bu-PPyV monomer emission to Bu-PPyV excimer emission as the dye content is increased. In devices without an electron transport agent, the maximum EL efficiency was 0.3%. By incorporating PBD to help transport electrons into these materials, the qualitative results were the same as a function of dye content, but the maximum efficiency was increased to 0.8% (Fig. 3). and the operating voltages were decreased (Fig. 4).

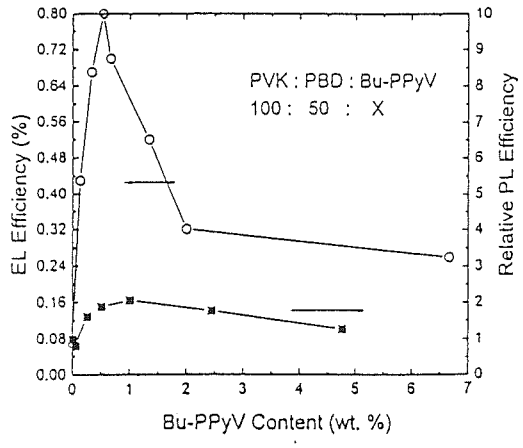

Fig. 3. External EL efficiency of ITO/PVK:PBD:Bu-PPyV/Mg:Ag/Ag devices and relative PL efficiency of the same organic films on glass [9].

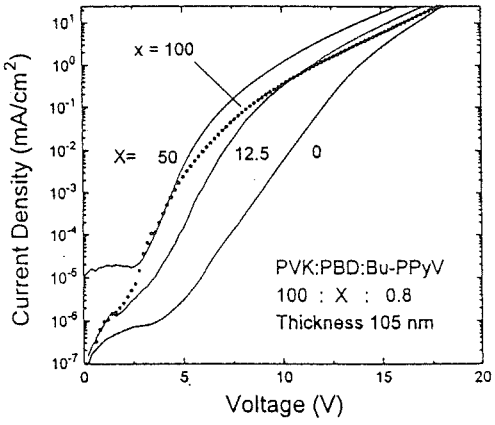

Fig. 4. Forward I-V characteristics of the ITO/Bu-PPyV/Mg:Ag/Ag devices for various PBD contents [9].

Note from Fig. 3 that the maximum relative increase in PL efficiency in the blends is only about two, while the EL efficiency increases by about a factor of 10 as the dye is added. Further, note that in devices under electrical excitation, already at 0.5 weight % dye, no emission from the PVK is visible (Fig. 2), whereas in PL at 1% weight % some PVK emission is still visible (Fig. 1). This leads us to conclude that excitons are formed on the dye under electrical operation by the sequential capture of electrons and holes, rather than exciton formation in the host followed by transfer to the dye [9]. The mode of operation of these devices is then shown in Fig. 5. Holes travel from the ITO through the PVK to be captured on the dye, and electrons travel from the cathode through the PBD to the dye.

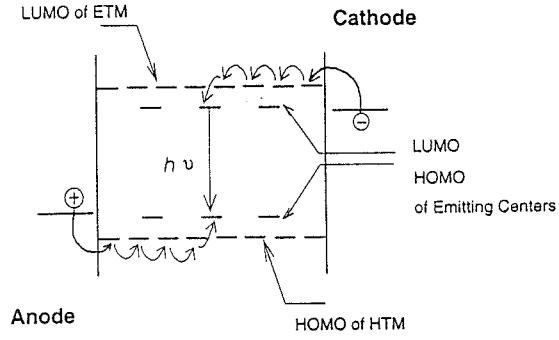

Fig. 5. Schematic diagram of carrier motion in single-layer devices consisting of a three-component organic layer.

To demonstrate the flexibility of doped single layer films for devices emitting different colors, we have also extensively used the dopants coumarin 47 (C47, blue), coumarin 6 (C6, green), and nile red (orange-red) in place of the Bu-PPyV. At 100 cm/m^2, external EL efficiencies of 0.5, 1.1, and 0.7% have been achieved at peak wavelengths of 450, 495, and 605 nm, respectively [9]. Fig. 6 shows the I-V and L-V curves for these three devices. Brightnesses of up to 10,000 cd/m^2 in DC operation are possible, and in some cases 100 cm/m^2 is possible in DC at less than 10 V drive condition.

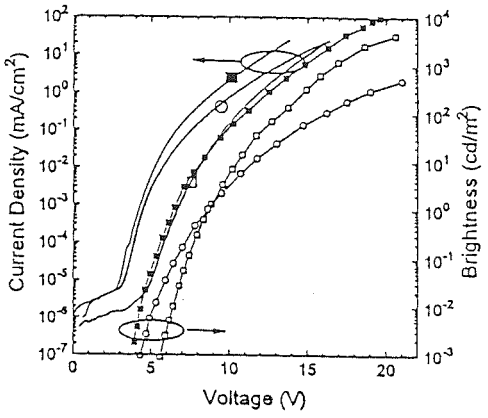

Fig. 6. Current-voltage-brightness characteristics of three component orange-red (open square), green (filled square), and blue (circle) single layer devices using nile red, C6, and C47 dyes [9].

ITO Surface Treatment

We have found that these single layer devices are extremely sensitive to the treatment of the ITO surface prior to the organic deposition. The ITO was purchased from a commonly used commercial vendor, and subjected to a series of sonification and solvent cleaning steps in our lab before a plasma treatment of the ITO surface before the organic deposition. Without a plasma treatment step, light emission did not begin until ~10 V, ~ 3 mA/cm^2 current densities required 20 V, the external quantum efficiency was 0.3%, and the maximum brightness before failure was ~300 cd/m^2. If an optimized oxygen plasma treatment was done to the ITO surface before the organic deposition [10], light emission began at 3 V, 3 mA/cm^2 current densities required <= 10V, the external quantum efficiency was raised to over 1%, and 10,000 cd/m^2 emission could be sustained (Fig. 7). In contrast to oxygen, hydrogen had a deleterious effect on the device performance.

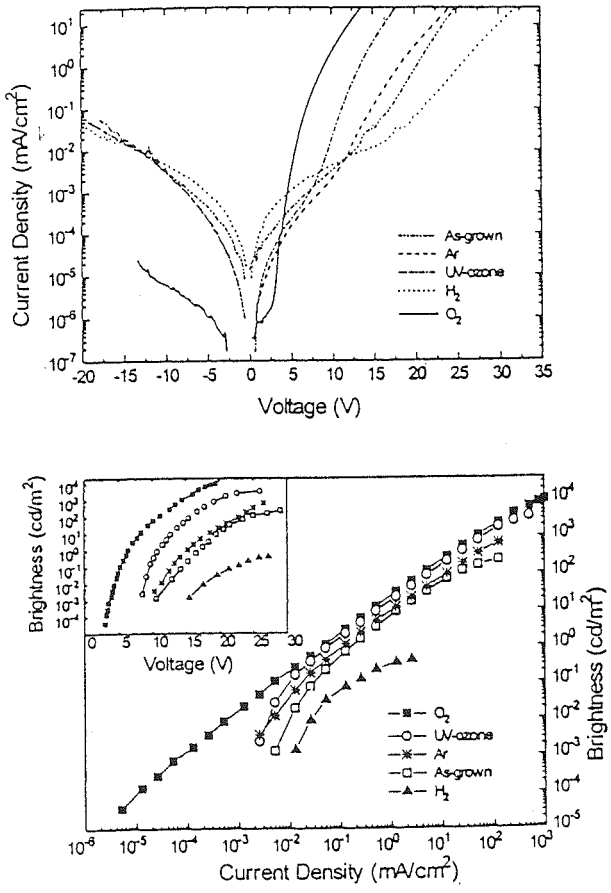

Fig. 7. I-V characteristics and brightness-current characteristics single layer ITO/PVK:PBD:C6/MgAg/Ag devices for various plasma treatments to the ITO surface before organic deposition. "As-grown" refers to no plasma treatment of the ITO. Detailed process conditions are in Ref. 10.

Because of the relatively mild plasma conditions used (25 W, room temperature, several minutes), the plasma did not induce bulk changes in the ITO (e.g. resistance, optical transmission, etc.) and its surface roughness as measured by AFM was not significantly changed. UPS

measurements of the ITO surface showed that the oxygen plasma did significantly increase the work function of the ITO (by 100-300 meV). This increase in the ITO work function decreases the barrier for hole injection into the organic materials, improving device operation. We believe this surface treatment is in large part responsible for the improvement in our device characteristics compared to results previously obtained in single-layer devices [1-6].

Multi-Color Integration

There are several approaches towards achieving full color OLED displays. These include shifting the color of devices by microcavities, using blue emitters followed by down-conversion modules to create red and green, and white emitters followed by color filter or a color tunable time-sequential shutter. All of these approaches sacrifice considerable amounts of energy compared to the optimum performance of individual blue, green, and red devices. The direct integration of OLED's of different organic layers onto a common substrate is difficult for two reasons. First, assuming a blanket deposition technique is used for the organic, one must pattern the organic layer in some way. An typical final desired structure is shown schematically in Fig. 8 (a.). In polymer LED's there is a second issue – once one of the devices in Fig. 8 (a.) has been created, spin coating of the second polymer will damage the edges of the first device through the dissolution of the first organic material by the solvent carrier of the second spin coating step. We have used the process structures of Fig. 8 (b.) and (c.) to overcome these problems.

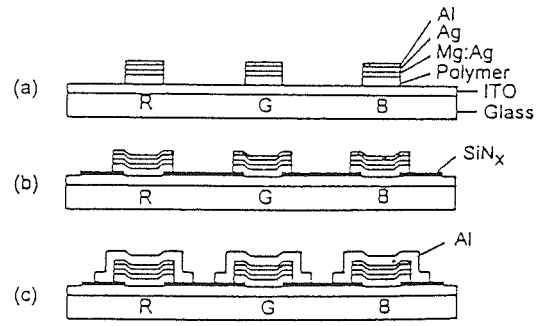

Fig. 8. Various integration structures for LED's with three different organics on the same substrate [11].

In the structure of Fig. 8 (b.), an insulating layer (e.g. silicon nitride) is patterned and deposited before the first organic deposition. This layer serves to render the edges of the devices electrically inert if they become damaged during processing. After a conventional spin coating step, the cathode contact is then deposited by evaporation through a shadow mask (Fig. 9.), which was aligned to cover the opening in the insulating nitride film. The metal cathode was then used as a mask to etch the organic blend layer using pure oxygen plasma. Dry-etching allowed the organic layer to be patterned without any undercutting or lift-off of the metal contact as could happen with wet etchants such as acids. Following plasma etching, the organic layer of the second LED was deposited by spin coating, completely covering the first LED. A second cathode contact was deposited by evaporation through a shadow mask, again followed by plasma etching. Note the etching of the second organic layer over the first LED was stopped by the metal cathode of the first LED. A third device was fabricated in a similar fashion.

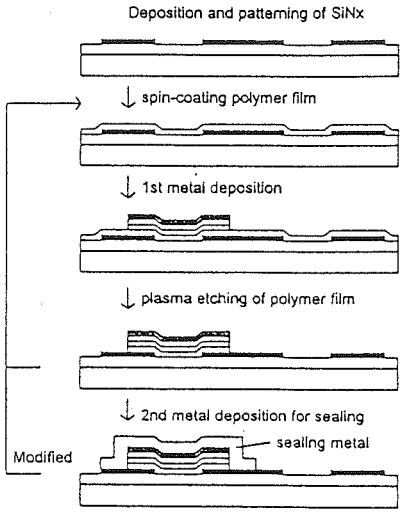

Fig. 9. Schematic process flow to integrate OLED's with multiple spin-coating steps onto a common substrate. The optional last step uses a second metal deposition step on each device to seal its edges to give the structure of Fig. 8 (c.).

The effect of processing on the devices was tested by comparing the characteristics of the first device right after its cathode was defined to those after the completion of the fabrication of all three devices. During this processing the first device was twice overcoated with other doped polymer layers which were removed by dry-etching. Fig. 10 shows that there was no measurable change in the device after such processing. The addition of a second metal evaporation step on each device allows the edge of the device to be "sealed" with an inorganic material. Using this process we have successfully integrated R,G, and B emitters onto a single substrate, all with performance comparable to those of the isolated devices of Fig. 6 [11]. In our work to date, the metal cathode patterns were defined by shadow masks, which has obvious limitations for large scale integration. Current work in our lab involves patterning the cathodes and LED's by photolithography.

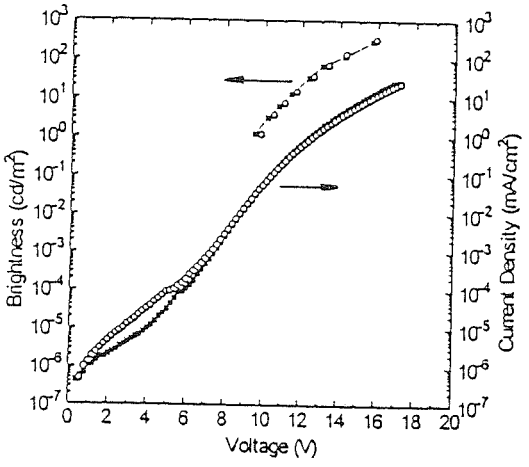

Fig. 10. I-V and L-V characteristics of an orange (nile red) single layer device before and after integration of blue and green devices.

Amorphous Silicon TFT Integration on Thin Stainless Steel Foils

Large matrix displays will require TFT's to be integrated with the OLED's to control their integration. Further, for lightweight flexible rugged displays, alternatives to glass are desirable. OLED's on plastic foils have been demonstrated by several groups. However, most plastic substrates have an upper temperature limit of about 200 °C, and the integration of TFT's requires about 300 °C. Therefore we have explored the alternative of very thin stainless steel foils (<= 200 um) as a substrate. Because of the thermal stability of stainless steel, amorphous silicon TFT's can easily be fabricated on these foils (coated with an insulating layer) with characteristics similar to those fabricated on glass [12].

The TFT process was a standard inverted staggered process similar to that in Ref. 12. The OLED was then fabricated using an Pt anode on the drain contact of the transistor. Because the steel is opaque, a semi-transparent cathode is required, to make a top emitting OLED. The doped-polymer thickness used was 140 nm, thicker than the usual 100 nm, because of some residual roughness from the steel. In early experiments ~15 nm Ag was used for the semi-transparent cathode, but better results [13] have been achieved using ITO sputtered at room temperature on top of a thin Mg:Ag layer (~10 nm) [14].

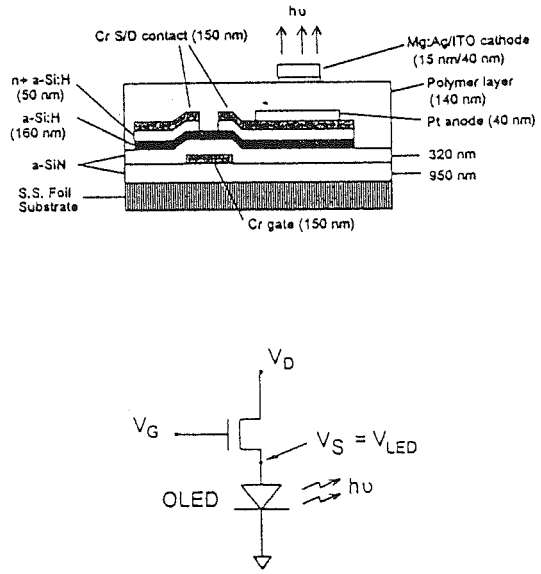

Fig. 11. Integrated TFT/OLED cross section and electrical circuit. The OLED diameter was 250 um and the TFT W/L ratio was 18. The organic layer was PVK:PBD:C6 (green emission).

The electrical circuit is a TFT in series with an OLED, in which the TFT gate voltage controls the current through the TFT and the OLED. The single-layer doped polymer OLED had an efficiency on the order of 0.1%, an order of magnitude lower than that usually achieved for similar bottom-emitting devices, presumably due to a non-optimized semi-transparent top contact. The drive voltage for display brightnesses was also ~20 V (compared to a usual 10V), probably due to the thicker organic layer. Nevertheless, holding the TFT drain at 40 V, changing the TFT gate voltage was able to switch the OLED on and off. A gate voltage swing of 20 V could switch the OLED from 0 to 50 cd/m^2, and from our results one can calculate that with an OLED efficiency of 1%, 100 cd/m^2 would easily be achievable with a gate voltage swing less than 10 V.

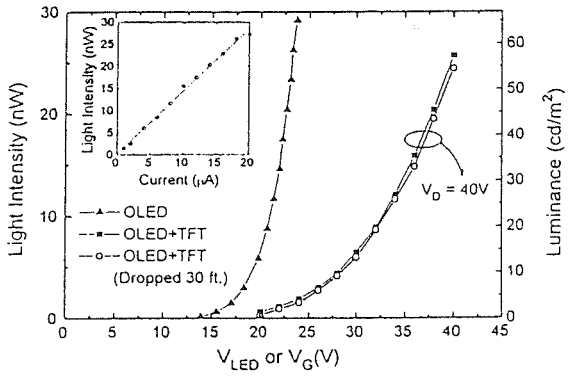

Fig. 12. Isolated LED characteristics (triangles, vs. V_{LED}) and integrated OLED/TFT characteristics (vs. V_G for V_D of 40 V) for the structure of Fig. 11 on 200 um stainless steel foils.

The ruggedness of the steel foils was demonstrated by dropping the finished circuits 10 m onto concrete, with no visible change in the device characteristics. The foils were also be flexed to a radius of 9 cm with the TFT and OLED operating with no noticeable change in device characteristics. Further work on thinner foils has shown that the bending radius with TFT's in operation

can be reduced to several mm, and will be reported elsewhere.

Summary

Doped polymer films allow the functions of electron transport, hole transport, and light emission to be individually optimized in single layer spin coated devices. These devices are very sensitive to ITO surface preparation, and an oxygen plasma treatment has a very beneficial effects. Dry processing allows one to integrate and pattern OLED's from multiple organic layers on a single substrate. Amorphous silicon TFT's can provide enough current to drive OLED's to display brightnesses, and thin stainless steel foils are an option for rugged lightweight substrates.

Acknowledgments

Collaborators on various parts of this project included S.D. Theiss, G. Gu, M.H. Lu, C.I. Wu, R. Register, M. Thompson, S. Wagner, A. Kahn, and S.R. Forrest. The work was supported by NSF, DARPA, and NJCST.

References

1. I.D. Parker, Q. Pei, and M. Marrocco, Appl. Phys. Lett. **65**, 1272 (1994).
2. C. Zhang, H. von Seggern, K. Pakbaz, B. Draabel, H.-W. Schmidt, and A.J. Heeger, Synth. Met. **62**, 35 (1994).
3. C. Zhang, H. von Seggern, B. Draabel, H.-W. Schmidt, and A.J. Heeger, Synth. Met. **72**, 185 (1995).
4. G.E. Johnson, K.M. McGrane, and M. Stolka, Pure Appl. Chem. **67**, 175 (1995).
5. J. Kido, M. Kohda, K. Okuyama, and K. Nagai, App. Phys. Lett. **61**, 761 (1992).
6. J. Kido, H. Shionoya, and K. Nagai, Appl. Phys. Lett. **67**, 2281 (1995).
7. J. Tian, C.C. Wu, M.E. Thompson, J.C. Sturm, and R.A. Register, Chem. Mat. **7**, 2190 (1995).
8. H. Tokuhisa, M. Era, T. Tsutsui, and [illegible] Saito, Appl. Phys. Lett. **66**, 3433 (1995).
9. C.C. Wu. J.C. Sturm, R.A. Register, J. Tian, E.P. Dana, and M.E. Thompson, IEEE Trans. Elec. Dev. **44**, (August, 1997).
10. C.C. Wu, C.I. Wu, J.C. Sturm, and A. Kahn, Appl. Phys. Lett. **70**, 1348 (1997).
11. C.C. Wu, J.C. Sturm, R.A. Register, and M.E. Thompson, Appl. Phys. Lett. **69**, 3117 (1996).
12. S.D. Theiss, IEEE Elec. Dev. Lett. **17** 365 (1996).
13. C.C. Wu, S.D. Theiss, G.Gu, M.H.Lu, J.C. Sturm, S. Wagner, S.R. Forrest, IEEE Elec. Dev. Lett., to be published, and C.C. Wu, S.D. Theiss, M.H. Lu, J.C. Sturm, and S. Wagner, IEDM Tech. Dig. 957 (1996).
14. G. Gu, V. Bulovic, P.E. Burrows, S. Venkatesh, Appl. Phys. Lett. **68**, 2606 (1996).